An evolutionary algorithm-based numerical material testing system based on a crystal plasticity finite element model

Koki Komatsu[1*] and *Tetsuo* Oya[1]

[1] Keio University, 3-14-1 Hiyoshi, Kohoku-ku, Yokohama 223-8522, Kanagawa, Japan

Abstract. Determining all necessary material parameters by simple material tests through numerical material testing method is effective for efficient forming simulation because it allows using complex material models with minimal effort. The proposed numerical material testing method is based on the concept of multi-scale virtual material testing with a crystal plasticity (CP) model. Since we use a crystal plasticity finite element model (CPFEM) of BCC materials, there are many microscopic parameters, including the non-Schmid parameter, as unknown variables. The CPFEM we use is a finite element polycrystal model (FEPM) based on the successive accumulation method to determine the activity of all slip systems. We have developed a numerical material testing system that uses an evolutionary algorithm to predict microscopic parameters from only a few in-plane tests. By learning work hardening-related parameters and texture-related parameters represented by Euler angles using in-plane test results as training data, the CP-based virtual material model acquires generalization capability and is able to predict unlearned biaxial test results with sufficient accuracy. The effectiveness of the proposed method is confirmed by simple forming simulations using the predicted material parameters.

Keywords: Numerical material testing; Forming simulation; Crystal plasticity; Optimization.

1 Introduction

Forming simulation has a major role in industry, but the increasing use of difficult-to-form materials requires phenomenological models. The use of this requires the acquisition of a large number of parameters from complex and numerous material tests to build phenomenological models.

Numerical material testing is a method of obtaining material data by conducting virtual experiments through numerical simulation [1]. This method has attracted attention and research as material models and forming simulations have become more efficient, as it avoids complex experiments and allows the necessary material parameters to be collected. In numerical material testing, the resolution of the constitutive equation representing the material is directly related to the accuracy of the analysis. Therefore, crystal plasticity finite element models which is using microscopic crystal plasticity [2,3] are expected to analyse the mechanical properties of materials by utilising microscopic mechanisms, which expresses dislocation theory, the physical behaviour inside single crystal, and linking it to the macroscopic world. Various validations based on same or similar ideas have been verified so far [4,5], and research is underway for practical applications.

Many crystal plasticity studies have been focused on FCC metal materials, and the methodology has not yet been established for BCC metals. The reason for this is that the deformation mechanism is more complex than that of FCC metals, with more slip systems [6,7], and it is difficult to construct a valid analytical model. However, there are many industrial applications of BCC materials, such as steel sheets for automobiles, and it is necessary to further investigate how to handle BCC materials in crystal plasticity models. In addition, research results have been reported on the use of discrete dynamics to represent the activity of BCC materials [8], but there is still a lack of research on how far it can be adapted and utilized by incorporating it into CPFEM.

The aim of this study is therefore to construct a model that more accurately represents the behavior of the BCC material ferrite in physical terms, and to show the process of numerical material testing with it. The accuracy of the model will be verified and the influencing factors on the anisotropy of ferrite will be further investigated. In the process of building these models, evolutionary strategies are used to calculate the necessary crystallographic parameters.

* Corresponding author : kokipine@keio.jp

2 Methods

The difficulty in constructing a CPFEM for BCC materials is that there is no established method for selecting slip systems and accurately representing the activity of each slip system. In BCC materials, unlike FCC materials, there are no truly close-packed planes, and multiple slip systems exist. It is known that the activity of these slip systems depends on temperature [9]. It has been reported that slip occurs on the [110] plane at low to room temperature, and activity occurs on the [112] plane at high temperatures [10, 11]. Therefore, in this study, a model was constructed using the slip system of the [110] plane.

As a method to accurately represent the activity of the slip system, the Non-Schmid law, which extends the Schmid law commonly used in CPFEM, was introduced and applied to a finite element polycrystalline model (FEPM) based on the sequential accumulation method.

2.1 Boundary condition

In crystal plasticity analysis, a representative volume element (RVE) is constructed to predict the macroscopic material response. In the analysis, each element represents a single crystal in the metal and for each element Euler angles (ϕ, θ, ψ) are given. This parameter describes the crystal texture. Each element is free to deform, but by applying appropriate boundary conditions to a virtual cube shown in Fig.1, where elements are aggregated sufficiently, the macroscopic material response can be obtained by homogenization. As for the number of elements, a mathematical homogenization with 1000 elements was found to be sufficient and the effect of stochastic errors was small, so it was adopted in this study.

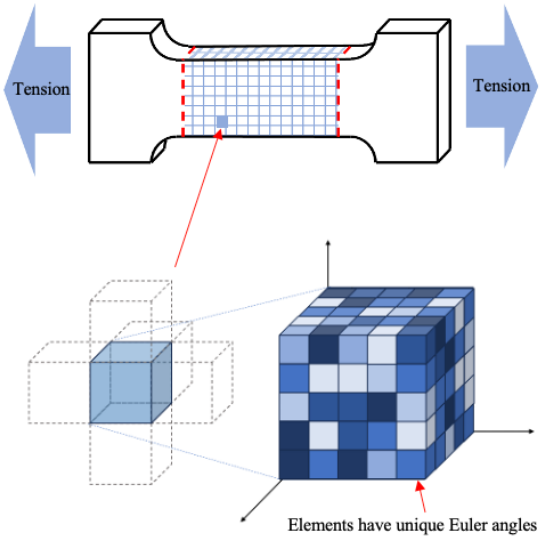

Fig. 1. Homogenisation image by RVE model.

To obtain reliable numerical material test results, the condition that the macroscopic work increment equals the total of the microscopic work increments must be satisfied [1]. To ensure this, the boundary conditions were given such that the displacements were periodic.

$$\begin{bmatrix} \dot{U} \\ \dot{V} \\ \dot{W} \end{bmatrix} = \boldsymbol{A} \begin{bmatrix} x \\ y \\ z \end{bmatrix},$$
$$\boldsymbol{A} = \begin{bmatrix} \dot{E_x} & \dot{E_{xy}}/2 - \dot{\Omega_{xy}} & \dot{E_{zx}}/2 - \dot{\Omega_{zx}} \\ \dot{E_{xy}}/2 - \dot{\Omega_{xy}} & \dot{E_y} & \dot{E_{yz}}/2 - \dot{\Omega_{yz}} \\ \dot{E_{zx}}/2 - \dot{\Omega_{zx}} & \dot{E_{yz}}/2 - \dot{\Omega_{yz}} & \dot{E_z} \end{bmatrix} \quad (1)$$

where $\dot{U}, \dot{V}, \dot{W}$ are the displacements corresponding to the x, y and z directions respectively, $\dot{E}$ is the macroscopic strain and $\dot{\Omega}$ is the macroscopic spin. They are calculated as the average of the microscopic values at every step. When analyzing the results of uniaxial tensile tests, rolling and shear, the analysis is carried out by giving conditions for these values to follow the respective conditions.

2.2 Successive accumulation method

In this study, a RVE model is constructed by introducing the successive accumulation method which proposed by Takahashi [12]. In contrast to the strain rate-dependent model generally used in crystal plasticity analysis, which does not directly determine the active slip system that causes crystal slip, the successive accumulation method determines the active or inactive slip at each step by successive calculation.

$$\chi_{(i)}^{(\gamma)} = \chi_{(i-1)}^{(\gamma)} + \left(\zeta^{(\gamma)}\tau^{(\gamma)} - k^{(\gamma)}\right)\frac{\Delta\rho}{2G} \quad (2)$$

where $\chi_{(i)}^{(\gamma)} = \zeta^{(\gamma)}\dot{\gamma}^{(\gamma)}$, $\zeta^{(\gamma)} = \mathrm{sign}\left(\tau^{(\gamma)}\right)$ and $\Delta\rho$ represents the step width of the iteration. Resolved shear stress $\tau^{(\gamma)}$is updated at each step and each slip increment in the next step is calculated from that value. A slip system for which $\chi^{(\gamma)} < 0$ during the calculation is judged inactive and the calculation continues with $\chi^{(\gamma)} = 0$. A slip system in which $\tau^{(\gamma)}$reaches the critical resolved shear stress $k^{(\gamma)}$ and $\chi^{(\gamma)}$ converges to a positive value is considered active. After these converge, the system updates by the hardening law from the increment and moves on to the next step of the calculation.

This equation can be used to carry out a plasticity analysis that physically faithfully represents the slip system. In the strain-rate-dependent modelling commonly used, the calculation accumulates displacement increments even for slip systems that

should not be sliding, except when the strain-rate sensitivity index $m = 0$. Numerical material tests are extrapolative predictions, as they aim to predict multiaxial stress states based on simple test results and to obtain parameters therein. Slip rate-dependent models that do not strictly capture the slip activity are not suitable for adoption in it. It is also problematic for wide application to a wide range of materials, as it only corresponds to strain-rate dependent cases. This method allows a strict determination of slip and thus avoids the use of m, and may be applicable to strain-rate-independent materials as well.

2.3 Non-Schmid law

In many CPFEM analyses, the Schmid law is assumed and the activity of the slip system is converted to macroscopic strain on the basis of this law. But the cases have been reported in which the Schmid law does not apply to BCC metals. It is reported as not only the stress component parallel to the direction of slip, but also other stress components influence the dislocation activity. In research on this issue, it has been reported that the Peierls stress, identified as the critical resolved shear stress acting parallel to the slip direction, is a function of both the orientation of the maximum resolved shear stress plane (MRSSP) and the magnitude of the shear stress perpendicular to the slip direction [13]. Taking this into account, Gröger et al. [14] and Koester et al. [15] extended the Schmid law by an analysis based on atomistic studies, leading to a method for calculating the effective driving force for slip. In addition to the general Schmid tensor $\boldsymbol{S_\alpha}$, the non-Schmid tensor $\boldsymbol{S'}_\alpha$, is added to calculate $\tau^{(\gamma)}$.

$$\begin{aligned}\boldsymbol{S'}_\alpha &= a_1\boldsymbol{m}_0^\alpha \otimes \boldsymbol{n'}_0^\alpha + a_2(\boldsymbol{n}_0^\alpha \times \boldsymbol{m}_0^\alpha) \otimes \boldsymbol{n}^\alpha \\ &+a_3\left(\boldsymbol{n'}_0^\alpha \times \boldsymbol{m}_0^\alpha\right) \otimes \boldsymbol{n'}^\alpha + a_4\boldsymbol{n}_0^\alpha \otimes \boldsymbol{n}_0^\alpha \\ &+a_5(\boldsymbol{n}_0^\alpha \times \boldsymbol{m}_0^\alpha) \otimes (\boldsymbol{n}_0^\alpha \times \boldsymbol{m}_0^\alpha) + a_6\boldsymbol{m}_0^\alpha \otimes \boldsymbol{m}_0^\alpha\end{aligned} \quad (3)$$

$$\tau^{(\gamma)} = \sigma : (\boldsymbol{S_\alpha} + \boldsymbol{S'}_\alpha) \quad (4)$$

where $\boldsymbol{m}_0^\alpha$ is the unit vector in the slip direction, $\boldsymbol{n}_0^\alpha$ is the unit vector perpendicular to the reference plane and $\boldsymbol{n'}_0^\alpha$ is the unit vector rotated in the negative 60◦ direction from $\boldsymbol{m}_0^\alpha$. a_1~a_6 are coefficients that indicate how much stress components other than those parallel to the slip surface affect the slip activity and differs rather from material to material. The a_1~a_6 shown in Table.1 , obtained by Koester's study [15], were used in this study.

Table. 1. The value of a_1~a_6 for BCC Iron [15].

a_1	a_2	a_3	a_4	a_5	a_6
0.61	0.23	0.55	0.11	0.09	-0.2

2.4 Model validation

A CPFEM for use in numerical material testing should accurately capture the physical behavior of the material based on its crystal structure. For the constructed crystal plasticity model to be able to represent the behavior of BCC materials, the results of uniaxial tensile tests of iron single crystals of various orientations were used to assess whether the deformation response of single crystal materials can first be predicted for single crystal activity. Various hardening laws for a crystal have been proposed for slip systems in crystal plasticity models. In this study Taylor's isotropic hardening model, which is expressed by the following equation, is used. Note, however, that the material parameters used in the past cannot be used as they are, due to the introduction of a slip system different from the CP model for FCC materials and the extension of the schmid law.

$$H(\Gamma) = \frac{\sigma^*}{M}\Gamma^n \quad (5)$$

Here, H is the shear stress of the slip system, Γ is the shear strain, and M is the Taylor factor. First, the initial σ^* and n values in Eq. (5) are crystallographic parameters and need to be determined on a material-specific basis. Since these two parameters cannot be measured experimentally, it is necessary to determine the appropriate parameters for the model through simulation. Therefore, the parameters were determined by an evolutionary strategy using the results of two uniaxial tests in the [011] and [111] directions as supervised data. A model using the parameters determined by the evolutionary strategy was used to verify whether the deformation response of the material in the [001] direction could be predicted by the model, and to further investigate the model. The genetic algorithm (GA) was used to extract each point of the experimental and analytical values, and their least squares error (RMSE) was minimized as the objective function.

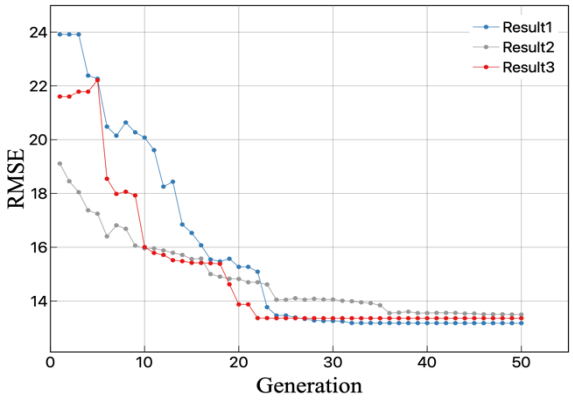

Fig. 2. Convergence curves of RSME for generations of GA.

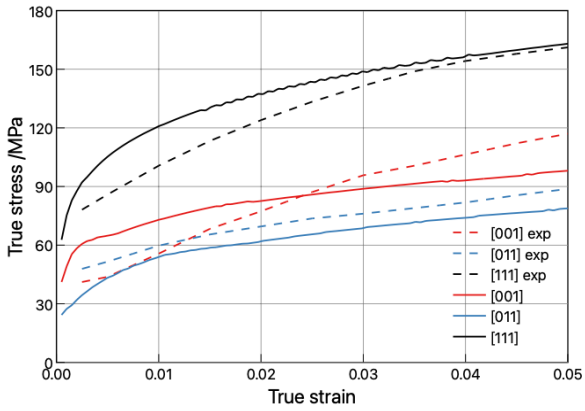

Fig. 3. Comparison of FEM and experiments in single crystal [15].

The GA process was run on 50 generations of 100 individuals based on the tournament method. The change in RMSE in the best individual of each generation is shown in Fig 2. The results of three trials are shown here to confirm the convergence of the GA.

All of these results are in convergence to a value where the RMSE remains Approximately 13. The possible causes of such errors include the possibility that the search by the GA was inadequate and did not fully explore the better results. Other possibility is that the research model developed itself did not have the expressive capacity to accurately reproduce both, and such errors are leaved as a limitation of the model. The results confirm that the decrease in values ended between 20 generation to 40 generations, and that the RMSE did not decrease with each subsequent generation, confirming that the GA converged to almost the same set. This suggests that the error is not due to inadequate exploration but to the inadequate representational capacity of the model.

The parameters determined here were used to analyze the [001] direction, and the results compared with the experimental values are shown in Fig. 3. In the optimized [011] and [111] directions, the analytical and experimental results are close. However, in the [111] direction, the approximation is not so good in the region of small strain. In the GA, the RMSE values converged as the generation increased; therefore, the differences are not due to insufficient optimization. Next, the results of the analysis in the direction [001] show that the values are closer as a whole than the experimental results, but the overall slope is different. The similarity in the slopes of the three analysis results in the [011], [111] and [001] directions, and the different slopes of the experimental data, indicates that there is still room for further investigation into the accuracy of the model and the parameterization method. The discrepancies can be attributed to the fact that many factors remain unexplored, such as the work-hardening model itself, the nature of the stress-strain curves that serve as supervising data and the optimization method, but the order of strength levels and the overall trend are reasonable.

3 Verification by polycrystal model

In this section, the FEPM is applied to polycrystalline materials to investigate whether the constructed model can be used as a numerical material test and to examine its accuracy. Here, the validation was carried out on SPCE, a cold-rolled steel material.

SPCE has a nearly constant stress-strain relationship and low anisotropy in uniaxial in-plane tension. Fig. 4 shows Uniaxial tensile tests in each in-plane direction (0°, 45°, 90°), the averaged data of which were used as the supervising data to relearn the crystallographic parameters of the FEPM. The resulting output results are also shown in Fig. 4.

3.1 Comparison by yield surfaces

A virtual in-plane test was conducted using the RVE model constructed in this study, resulted in the yield surface shown in Fig 5. The experimental data in the figure is based on the results of Kuwabara [17] for SPCE. It was plotted where the equivalent plastic strain ε_p = 0.001. For comparison, a model (corresponding to an FCC material) is also included here, which does not introduce the Non-Schmid law and adopts the [111] system, which is the slip system of the FCC. It can be seen from Fig. 5 that the proposed model is able to represent the yield function of the SPCE better than the conventional one. This improvement in accuracy can be attributed to the introduction of the Non-Schmid law, which allows the stress components contributing to slip to be treated accurately.

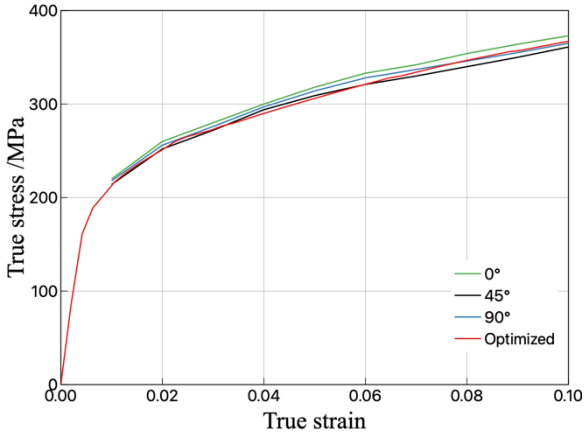

Fig. 4. Stress-strain curves and calculation results for SPCE [16].

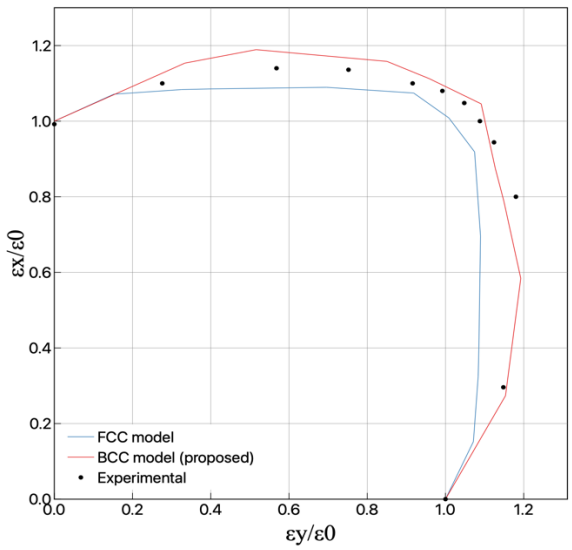

Fig. 5. Normalized yield surfaces obtained by the experiment [17] and calculated by CPFEM models with FCC and BCC representation.

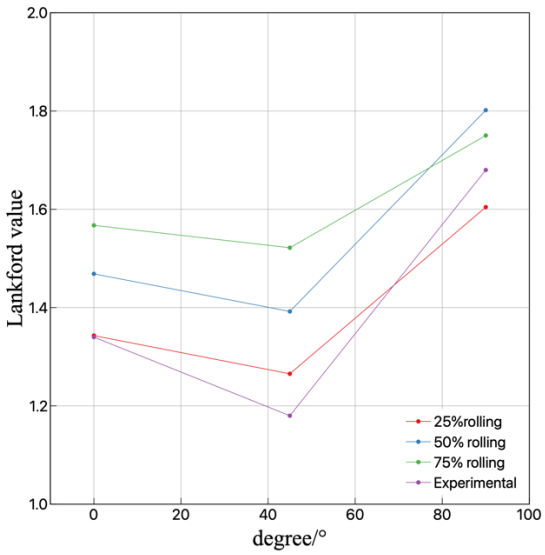

Fig. 6. Lankford values for different compression rate of numerical rolling [16].

3.2 Deformation anisotropy prediction by numerical rolling

The expression of the hardening and anisotropy of the material in the CPFEM of this study is by the parameter in the hardening law shown in Eq. (5) and the Euler angles given to each element, which represents the crystalline aggregate structure. Therefore, in order to obtain information on the aggregate microstructure of the rolled SPCE material, numerical rolling was carried out to obtain the Euler angles for each element. In numerical rolling, rolling is carried out virtually on the model by fixing the y-directional displacement in Eq. (1) and compressing it from the z-axis direction. Therefore, if compression is done from the z-axis for each displacement rate $\dot{e}$ at each step, the boundary condition is as follows.

$$\dot{E_x} = \frac{-\nu}{1-\nu}\dot{e} + \frac{1-2\nu}{1-\nu}\dot{\varepsilon_x^p}, \dot{E_y} = 0, \dot{E_z} = -\dot{e} \qquad (6)$$

where, ν is Poisson's ratio and $\dot{\varepsilon_x^p}$ is the x component of the plastic strain rate. However, the compression rate is unknown for the hypothetical aggregate structure of SPCEs by numerical rolling. Therefore, compression rates of 25%, 50% and 75% were prepared for verification purposes.

The r-values (Lankford values) of the rolled sheets were calculated using these rolled FEPM model. The results and the experimental values for comparison are shown in Fig 6. The results confirm that anisotropy develops as rolling proceeds, and that numerical rolling can create a collective structure. It was also confirmed that the r-values for the 25% rolling were close to the experimental [16] values compared in this study. For those with 75% rolling, the r_{90} value was found to be lower than at 50%. This may be due to the higher rolling rate, which may have increased the deformation of the RVE model, and the influence of some elements on the overall deformation. In addition, different r-values for SPCE have been reported in the literature [18], and they vary somewhat depending on the experimental environment and conditions. However, it has been found that there is a similar trend with regard to its strength ranking, with a larger value of r_{90} compared to r_0 and r_{45}. On this basis, it can be said that the collective microstructure obtained by this numerical rolling captures the feature of a larger r_{90}, and thus generally captures the material anisotropy of the SPCE.

3.3 Confirmation by forming simulation

In order to validate the accuracy of the prediction of material deformation from the values obtained from the numerical material tests performed by the proposed model, forming simulations were performed in this section using the values calculated in this study. From the results obtained, LS-DYNA was used to simulate the cup-drawing forming for SPCE. A schematic diagram of the model is shown in Fig. 7. A plastic anisotropic yield function of Hill48 was used based on r-values calculated at two compression rates, 25% and 50%, which are considered to reflect the anisotropy of the SPCE relatively well. The analysis model was set up and simulated according to the conditions presented by Wu et al. [18]. to compare the results with the cup-edge profile.

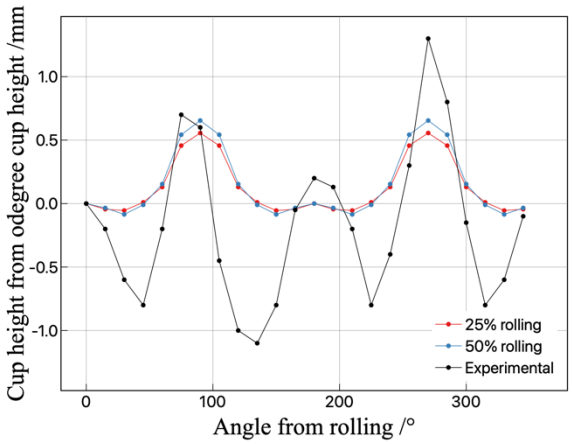

Fig. 7. Comparison of cup-height profiles for different compression-rate of numerical rolling with experimental result by Wu et al. [18].

A comparison of the edge profiles obtained as a result of the analysis and the profiles obtained as a result of the experiment by Wu et al. [18] is shown in Fig7. The results show that the analysis based on the *r*-values obtained from the present material tests is able to capture the feature of higher cup edges in the 90° direction, but not the reduction in height in the 45° direction.

This could be improved by improving the accuracy of the analytical aspects, such as utilizing other macroscopic anisotropic yield functions instead of using the Hill48 model, which is a concise form in forming simulation, and by introducing non-associated flow rules.

4 Conclusions

In this study, a model introducing the Non-Schmid law was constructed to extend the numerical material testing method based on FEPM to BCC materials, and a basic study on the model and parameter determination method was conducted. By utilizing the GA, crystallographic parameters that could not be determined from the tests could be determined, thereby allowing the model to be constructed.

Compared to conventional models, the model reproduced the material response of BCC single crystals and, in comparison with polycrystalline materials, predictions about the yield surface and *r*-values of SPCE could be made only from the results of uniaxial tensile tests. However, the quantitative accuracy of the values remained an issue.

In aiming to improve accuracy in the future, as mentioned earlier, changes to the hardening rule may be a way to achieve this. In this study, Taylor's isotropic hardening law was used for brevity, but there is room for improvement here. Further improvements in accuracy can be expected in the future by utilizing an anisotropic hardening law that gives a yield function for each slip, or by incorporating its interaction matrix. Also, as for numerical rolling, a method to obtain a more accurate texture would lead to a more quantitative evaluation of material anisotropy.

References

1. T. Oya, N. Araki, Mater. Today Commun., **33**, 103953(2022)
2. J. Pan, J.R. Rice, Int. J. Solids Struct., **19** (11) (1983)
3. D. Peirce, R.J. Asaro, A. Needleman, Acta Metall., **31**-12(1983)1951.
4. M. Kraska, M. Doig, D. Tikhomirov, D. Raabe, F. Roters, Comput. Mater. Sci., **46**-2(2009) 383.
5. H. Zhang, M. Diehl, F. Roters, D. Raabe, Int. J. Plast. **80** (2016) 111.
6. A. Seeger, Mater Sci Eng A., **319-321**(2001), 254.
7. J. W. Cristian, Metall Trans, **14**(1983)1237.
8. R. Madec, L. P. Kubin, Acta Mater, **26**(2017)166.
9. D. Brunner, J. Diehl, Phys Stat Sol(a), **124**(1991) 455.
10. D. Caillard, Acta Mater., **58**(2010)3493.
11. D. Caillard, Acta Mater., **58**(2010)3504.
12. H. Takahashi, K. Fujiwara, T. Nakagawa, Int. J. Plast,. **14** (6) (1998) 489.
13. R. Gröger, A.G. Bailey, V. Vitek Acta Mater., **56**(2008)5401.
14. R. Gröger, V. Racherla, J.L. Bassani, V. Vitek Acta Mater., **56**(2008)5412.
15. A. Koester, A. Ma, A. Hartmaier, Acta Mater., **60**(2012)3894.
16. K. Naruse, B. Dodd, Y. Motoki, Transactions of the JSME A, **57**-543(1991)2659.
17. T, Kuwabara, Tetsu-to-Hagané, **108**-4(2022)233.
18. B. Wu, K. Ito, N. Mori, T. Oya, T. Taylor, J. Yanagimoto, Int. J. Precision Eng. and Manuf., **7**(2020)465.